Journal of Power Sources 231 (2013) 106–112

Contents lists available at SciVerse ScienceDirect

Journal of Power Sources

journal homepage: www.elsevier.com/locate/jpowsour

Composite-coated aluminum bipolar plates for PEM fuel cells☆

Jennifer R. Mawdsley [a,*], J. David Carter [a], Xiaoping Wang [a], Suhas Niyogi [a], Chinbay Q. Fan [b], Rasit Koc [c], George Osterhout [d]

[a] Chemical Sciences and Engineering Division, Argonne National Laboratory, 9700 S. Cass Ave., Lemont, IL 60439, USA
[b] Gas Technology Institute, 1700 S. Mount Prospect Road, Des Plaines, IL 60018, USA
[c] Department of Mechanical Engineering and Energy Processes, Southern Illinois University Carbondale, 1230 Lincoln Dr., Carbondale, IL 62901, USA
[d] Orion Industries, 5170 North Northwest Highway, Chicago, IL 60630, USA

HIGHLIGHTS

► TiC and graphite were identified as the best conductive filler powders.
► 3000 series Al alloys have the best corrosion resistance under fuel cell conditions.
► Composite-coated Al meets the DOE cathodic electrochemical corrosion target.
► Composite-coated Al performs better in a single cell stack than uncoated Al.

ARTICLE INFO

Article history:
Received 28 September 2012
Received in revised form
13 December 2012
Accepted 17 December 2012
Available online 24 December 2012

Keywords:
Bipolar plates
Fuel cells
Coatings
Aluminum
Corrosion

ABSTRACT

Aluminum-based bipolar plates for proton exchange membrane (PEM) fuel cells offer high strength and durability while weighing up to 65% less than stainless steel. To protect the aluminum from electrochemical corrosion while maintaining electrical conductivity, coatings that are a composite of a fluoropolymer and one or more conductive inorganic fillers were investigated. Titanium carbide (TiC) and graphite were found to be the best candidates for conductive fillers among six powders that were tested for acid and electrochemical stability. Composite coatings of graphite, TiC, and ethylene-tetrafluoroethylene (ETFE) were applied to the aluminum or ceramic substrates by wet spraying followed by heat treatment, and then tested for in-plane sheet resistance, through-plane area specific resistance (ASR), electrochemical corrosion resistance, flexural strength, and flexibility. The composite-coated aluminum plates meet the U.S. DOE targets for bipolar plates for in-plane conductivity, flexural strength, and cathodic corrosion resistance. The targets for through-plane ASR and anodic corrosion resistance were not met due to the spraying process producing an undesirable layered microstructure and also a microstructure with connected porosity and pinholes.

1. Introduction

Aluminum bipolar plates for proton exchange membrane (PEM) fuel cells offer potential cost, volume, and weight reductions as compared to the currently used machined graphite bipolar plates, while also offering improved mechanical properties. As compared to stainless steel, aluminum is up to 65% lighter in weight with negligible difference in cost per unit volume. This magnitude of potential weight reduction has obvious advantages in transportation applications because there are 740 bipolar plates in each automotive PEM fuel cell stack [1]. Furthermore, aluminum is the only practical alternative metal to stainless steel for PEM fuel cell bipolar plate applications due to the high cost of titanium [2], the poor formability of Mg alloys [3], the toxicity of Be, and the reactive properties Li, Na, Ca, and K.

Pure, oxide-free aluminum can meet all of the DOE bipolar plate targets [4] except for corrosion resistance. To overcome this one weakness, we have applied a composite coating consisting of a matrix of an acid-resistant fluoropolymer and a filler material that is electrically conductive and acid-resistant. Our approach

☆ The submitted manuscript has been created by UChicago Argonne, LLC, Operator of Argonne National Laboratory ("Argonne"). Argonne, a U.S. Department of Energy Office of Science laboratory, is operated under Contract No. DE-AC02-06CH11357. The U.S. Government retains for itself, and others acting on its behalf, a paid-up nonexclusive, irrevocable worldwide license in said article to reproduce, prepare derivative works, distribute copies to the public, and perform publicly and display publicly, by or on behalf of the Government.

* Corresponding author. Tel.: +1 847 971 1144; fax: +1 630 985 0555.
E-mail address: jennifermawdsleyphd@gmail.com (J.R. Mawdsley).

0378-7753/$ – see front matter © 2013 Elsevier B.V. All rights reserved.
http://dx.doi.org/10.1016/j.jpowsour.2012.12.074

combines the advantages of metallic plates – high bulk electrical conductivity, high mechanical strength, extremely low hydrogen permeation – with the advantages of polymer-inorganic composites – lower contact resistance and good corrosion resistance [2]. Wet spraying was chosen as the method to apply the coatings to the aluminum substrates because it is a widely accepted industrial process already used for many consumer goods.

To develop the composite-coated bipolar plates, preliminary experiments were first conducted to determine which filler materials would be the most acid resistant. Also, a preliminary study of the electrochemical corrosion resistance of various commonly available aluminum alloys was performed. Then composite coatings were sprayed onto 6061 and 3003 aluminum alloys to determine which compositions yielded the highest electrical conductivities. Once a suitable composition was determined, mechanical properties and electrochemical corrosion tests were conducted. Finally, aluminum bipolar plates stamped with gas flow channels were coated and tested in a two-plate, one cell stack.

2. Experimental details

2.1. Acid stability tests of candidate filler materials

Six candidate filler powders were tested for stability in sulfuric acid at 80 °C. This was done because other published data for acid stability tests were not conducted at the correct temperature and often for short durations (<2 days) [5]. The six powders tested were graphite (Superior Graphite LGB2025), LaB_6 (Aldrich), $TiSi_2$ (Aldrich), TiC [6,7], TiB_2 [8,9], and CaB_6 [10]. These six compositions were chosen because they were reported to have high electrical conductivity and good acid resistance [5]. The acid stability tests were conducted with sulfuric acid solution that was 0.001 M H_2SO_4 with 0.1 ppm NaF (pH = 3). This is the same as the solution recommended by the DOE for bipolar plate corrosion test [4]. Studies indicate that concentration of sulfate ions in PEMFC effluent is low[11], so the 0.001 M solution simulates real conditions in a PEM fuel cell. In the experiment, ~0.35 g of powder was immersed in 100 mL of the prepared acid solution and heated to 80 °C in a round bottom quartz flask under flowing 3.5% H_2 in He for 27–33 days. A chilled condenser column was used to prevent the acid vapors from escaping. After the experiment was over, the acid was filtered from the powder. The powder was rinsed three times, dried overnight and then weighed. This value was used to calculate how much powder was retained. The powder was then characterized by X-ray diffraction (Siemens D5000) to detect new phases. The acid that was filtered was analyzed using induction coupled plasma-optical emission spectrometry (ICP-OES) to detect dissolved cations (Ti, La, Ca, B, and Si).

2.2. Electrochemical stability tests of candidate filler materials

Four candidate filler samples, CaB_6 (Alfa Aesar), TiB_2 (Cerac), $TiSi_2$ (Aldrich), and TiC (SIU and Aldrich) were tested using the thin film rotating disk electrode (TF-RDE) technique in 0.1 M H_2SO_4 at room temperature. The purpose of this experiment was to screen for the most stable candidate filler by comparing the relative electrochemical stability of these samples in 0.1 M H_2SO_4 solution at room temperature. Sulfuric acid solutions with concentrations ranging from 0.05 to 1.0 M H_2SO_4 have typically been used for electrochemical experiments to accelerate corrosion and minimize electrolyte resistance [12–15].

The commercially produced powders were first ball milled to reduce particle size, while the powder from SIU was used as-received. The powder samples were made into an ink by mixing with Nafion® solution and organic solvent. The volume ratio of the powder to dry Nafion® was 50:50. The loading of power on the RDE was 155 μg cm^{-2}. During the electrochemical testing, both cyclic voltammetry with potential range of 0–1.0 V and chronoamperometry for 1 h were used to characterize the samples either in oxygen saturated or Ar purged electrolyte. The electrochemical characterizations performed in both oxygen saturated and Ar purged electrolyte allow determining the influence of the presence of oxygen on the redox behavior of the samples.

2.3. Sample fabrication

The coatings contained 30–60 vol% ETFE (Fluon, Asahi Glass Co.) as the fluoropolymer and 20–70 vol% flake graphite (LBG2025, Superior Graphite) and/or 10–30 vol% titanium carbide as the filler. The titanium carbide powder (TiC) was prepared using a carbothermal reduction process [6,7] which resulted in nano-size grains that were agglomerated into large, high surface area structures. Coating slurries were made by mixing the starting powders with solvents (2:1 *o*-xylene:diisobutylketone by volume) and ball milling with YSZ media until a stable suspension was achieved. A bond coat anchor polymer was synthesized [16], dissolved in tetrahydrofuran, and mixed with carbon black (Cabot, Vulcan XC-72). A very thin layer (<100 nm) of this suspension was first sprayed on the grit blasted 6061 or 3003 aluminum substrates using an airbrush. This was following by spraying of the coating suspension using multiple passes to build up a layer of the desired thickness, drying the coating in air at room temperature, and then sintering the fluoropolymer to form a continuous coating at 310 °C for 3 h in ambient air. For the in-plane electrical resistance measurements, an aluminum oxide substrate was used instead of aluminum. For the corrosion, flexure tests, and single MEA tests, samples on 3003 aluminum were made in a similar manner using wet spraying at Orion Industries, except the bond layer was not applied to these substrates.

2.4. Though-thickness electrical resistance measurements

Resistivity measurements were conducted according to the methods published by Wang et al. [17] and Avasarala and Haldar [18]. Aluminum samples were sandwiched between two pieces of carbon paper (Toray), and two copper disks. Leads were attached to the copper disks and the assembly was placed in a Carver press with a self-leveling platen. Load was applied (142 N cm^{-2}) and the resistance was measured using a potentiostat (Princeton Applied Research model 273A). The resistance of the system without a sample was subtracted from each measurement. The area specific resistance (ASR) was calculated by multiplying by the area of the carbon paper.

2.5. In-plane electrical resistance measurements

The in-plane electrical conductivity was measured using a 4-point probe (Jandel) connected to a potentiostat (Princeton Applied Research model 273A). This measurement was done on the films sprayed onto ceramic substrates because the method is not valid for films on conductive substrates. To run this test, samples were placed under the 4-point probe and the probe lowered so all four points touched the top surface of the sample. A galvanodynamic signal (0.1 to −0.1 A to 0.1 A at 0.01 A s^{-1}) was then passed through the sample and the voltage generated was measured. The sheet resistance is the slope of the resulting *I* vs. *E* graph.

2.6. Flexure testing

Flexural strength and flexibility of the composite-coated aluminum coupons were determined with 3-point bending tests

using a mechanical testing machine (Instron model 4505). These tests were carried out in accordance with ASTM standard D790. The samples used were cut from a coated panel made by Orion Industries where the coating was 25 vol% graphite, 25 vol% TiC, and 50 vol% ETFE. The sample dimensions were 76.3 mm long × 13 mm wide × 1 mm high. The cut sides of each sample were polished and chamfered using 600 grit SiC paper. The test fixture had a support span of 3 cm. The crosshead traveled at a speed of 0.11 mm/min, as prescribed by ASTM standard D790.

2.7. Electrochemical corrosion measurements

For the electrochemical corrosion tests, either an uncoated aluminum alloy sheet or a composite-coated 3003 aluminum sample was clamped beneath an open glass cylinder test cell (PTC1, Gamry) with a grooved flange on the bottom that used a fluorosilicone o-ring (McMaster-Carr) to create a seal. The test conditions used were based on those described in the U.S. DOE targets for bipolar plates [4]. Thus, the glass cylinder was filled with 0.001 M sulfuric acid with 0.1 ppm NaF (pH = 3). The top of the cylinder was sealed with a rubber stopper through which there were fed two tubes to bubble air or argon into the acid solution, as well as a reference electrode (Ag/AgCl, Gamry), a graphite rod counter electrode, and a PTFE-coated thermocouple. This test fixture was put into a sand bath and heated to 80 °C. The leads of a potentiostat (Solartron Analytical 1480) connected to a frequency response analyzer (Solartron Analytical 1252A) were attached such that the sample acted as the working electrode in a 3-lead type of experiment. For tests conducted under cathodic conditions, air was continuously bubbled through the acid solution and 0.6 V vs. Ag/AgCl (or 0.8 V vs. NHE) was applied for 24–48 h. For tests conducted under anodic conditions, argon was continuously bubbled through the acid solution and −0.4 V vs. Ag/AgCl (or −0.2 V vs. NHE) was applied for 24–48 h. An argon purge is specified in the DOE targets because it deoxygenates the electrolyte solution more effectively. As the sulfuric acid solution evaporated, it was replaced with fresh solution supplied by a syringe pump.

2.8. Single MEA testing

3000 series aluminum sheets were stamped with a propriety flow field design and then welded together back to back to create internal cooling channels. The design is based on a patented trapezoidal flow field structure for PEM fuel cells with very low pressure drop [19]. The exterior flow channels were 760 μm deep and the active area was 60 cm^2. The stamped and welded plates were coated with a composite coating by Orion Industries. A single MEA (Gore) was sandwiched between two bipolar plates and sealed with a polyurethane gasket. This was mounted inside a test stand and tested at 50 °C with H_2 and air inputs.

2.9. Scanning electron microscopy

Scanning electron microscopy (SEM) was conducted using a JEOL JSM-6400 and a Hitachi S4700. To prepare the composite-coated specimens for SEM, selected samples were cut to reveal the coating cross-section, mounted in epoxy (Buehler), and then vibratory polished with SiC grit paper followed by 1 μm alumina polishing powder on a kerosene-soaked polishing cloth (TexMet 1000, Buehler). Loose powders were prepared for SEM simply by sprinkling a small amount onto a double-sided adhesive carbon tab mounted on an aluminum SEM stub.

3. Results and discussion

3.1. Acid stability experiments

The results of the experiment are shown in Table 1. The results given in the "% Sample Remaining" column were calculated from the weight change measurements. There is some error due to powder not recovered because a small amount of it was stuck to the stirbar and on the filter paper, however, it is estimated to be under 1% of the original mass of the powder.

It can be seen clearly in Table 1 both TiC and $TiSi_2$ gained weight, which is an indication of the powder reacting with the acid to form a secondary phase rather than dissolving. Powder X-ray diffraction results showed the presence of small amounts of both metallic silicon (Si) and titanium monosilicide (TiSi) in the as-received $TiSi_2$ powder. In the reacted $TiSi_2$ sample powder X-ray diffraction pattern, both secondary phases were present, but there were also peaks from two forms of titanium oxide, TiO_2 and Ti_3O_5. ICP-OES analysis of the sulfuric acid solution from the $TiSi_2$ experiment showed the presence of 156 mg L^{-1} of Si and <0.6 mg L^{-1} of Ti. (Note: the Si level from the experiment with graphite was only 1.14 mg L^{-1}.) We deduced that at least some of the dissolved Si had to be from a Ti-containing phase because Ti oxides were found. This indicates that the $TiSi_2$ is breaking down in the sulfuric acid and that the Si remains in solution while the Ti is precipitating out. For the TiC, no extra phases were found in XRD, so we assumed that the weight gain is due to contamination. Both of the borides released boron into the acid. In the case of TiB_2, this resulted in the formation of oxides and sulfates. The Ca in the CaB_6 also dissolved into the solution. ICP-OES cannot detect carbon in the solution, so it is unknown if the graphite weight loss was due to some graphite sticking to the filter or partial dissolution. From these tests, we concluded that TiC and graphite were the most acid stable.

3.2. Electrochemical stability experiments

Table 2 gives the summary of the results of the TF-RDE electrochemical corrosion experiments on candidate filler powders. Based on the corrosion current values shown in Table 2, $TiSi_2$ appears to be the best candidate filler material among those samples tested. However, the corrosion current is high enough to indicate a potential reaction if the test was carried out for a much longer time period, as was done in the acid stability experiments discussed in Section 3.1. The TiC samples also appear to have been more corrosion resistant than the two metal boride materials that were tested. The TiC was acceptable, but a small oxidation peak at 0.56 V occurred when cathodic scan went to a potential less than 0.4 V. Since these tests were performed at room temperature there are some differences from the acid stability experiments. When the results from the two tests are taken together, the TiC was chosen as

Table 1
Acid stability of candidate filler powders.

Sample	Time (days)	% Sample remaining	Extra phases in XRD	Ion concentration (mol L^{-1})
TiC	32	109	None	Ti: n.d.
Flake graphite	33	94	None	Si:
$TiSi_2$ (with TiSi and Si impurities)	30	132	Ti_3O_5, TiO_2	Ti: n.d., Si: 5.6×10^{-3}
LaB_6	31	81	None	La: 3×10^{-4}, B: 1.7×10^{-3}
TiB_2	27	95	TiO_2, H_2BO_2, $TiOSO_4$	Ti: n.d., B: 9.0×10^{-2}
CaB_6	31	92	None	Ca: 5.0×10^{-3}, B: 1.4×10^{-2}

Table 2
Rotating disk electrode electrochemical stability of candidate filler powders.

Sample	Corrosion current (A cm^{-2})			Observations from cyclic voltammetry
	0.84 V in Ar	0.84 V in O_2	0.14 V in Ar	
TiC (SIU)	6.24×10^{-6}	1.34×10^{-5}	7.06×10^{-6}	A small oxidation peak at 0.56 V occurred when cathodic scan went to a potential less than 0.4 V.
TiC (Aldrich, milled)	4.92×10^{-5}	2.87×10^{-5}	2.27×10^{-5}	Same features as for unmilled SIU TiC
$TiSi_2$	5.65×10^{-6}	5.70×10^{-6}	4.75×10^{-6}	No obvious redox features
TiB_2	1.11×10^{-5}	9.41×10^{-6}	7.08×10^{-6}	An initial oxidation current in the entire potential range (0–1.0 V) gradually decreased until stable CV occurred.
CaB_6	2.44×10^{-5}	2.47×10^{-5}	-3.31×10^{-5}	Initial CV showed an oxidation peak at 0.46 V

the best candidate along with graphite and carbon black for the filler phase in the composite coatings.

3.3. Electrochemical corrosion resistance of various aluminum alloys

Electrochemical corrosion tests were conducted on various uncoated aluminum alloys to determine which were best suited for use in a PEM fuel cell. The results from the tests conducted under cathodic conditions are shown in Fig. 1 and Table 3, while the results from the tests conducted under anodic conditions are shown in Fig. 2 and Table 4. A higher current density corresponds to a higher corrosion rate. Overall, the anodic conditions were more corrosive to the aluminum alloys that the cathodic conditions. Anodic conditions similar to the ones used in these tests are commonly used to anodize aluminum, so the higher corrosion currents in anodic mode were not surprising. All samples showed signs of oxide formation on the surface in the form of discrete spots, a sign of pit corrosion. These oxide regions increase the through-plane resistance of the plates, which is undesirable for bipolar plate applications. Sheet resistance measurements after corrosion testing show that 3003 and 6061 were the least oxidized under cathodic conditions and 3105, 2024, and 3003 were the least oxidized under anodic conditions. The 3003 aluminum had the best combination of low cathodic and anodic current density, while the 5052 aluminum was the worst performer. The manganese in the 3000 series aluminum alloys may be responsible for the good performance because it helps form a protective oxide surface [20] that may also have properties similar to chromate conversion coatings [21]. Thus, 3000 series aluminum was chosen as the substrate for all of our electrochemical corrosion and single MEA testing.

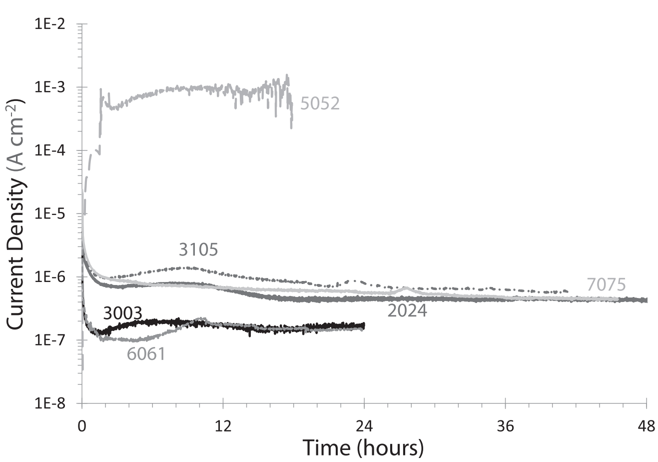

Fig. 1. Electrochemical corrosion test results for various uncoated aluminum alloys under simulated cathodic PEM fuel cell conditions.

3.4. Electrical resistance of composite coatings

The measured electrical conductivities of the composites, Table 5, were significantly lower than the published bulk conductivities of the fillers likely because the fluoropolymer may act to separate the filler particles as it flows between the particles during sintering. As shown in Table 5, the ASR of the composite coating decreased when the part of the graphite in the coating was substituted with TiC. The TiC helps to increase the through-thickness conductivity by filling in the space between the graphite, as shown in the SEM micrograph in Fig. 3. The TiC nanoparticles are agglomerated in a way, Fig. 4, such that they can provide a conduction path between the graphite flakes while still allowing enough fluoropolymer in the microstructure to provide adhesion and flexibility. We found that a ratio of graphite to TiC of 5:1 was better than 1:1 for both through-thickness and in-plane resistance. For the in-plane sheet resistance the data indicates having the graphite plates aligned on the surface and having more of it lowers the sheet resistance as would be expected. The samples with more TiC had a much higher sheet resistance indicating the microstructure of the TiC gives a more resistive surface even though TiC itself has a higher conductivity than graphite [5,22]. It is likely that the more spherical morphology of the TiC produces a surface with a higher proportion of non-conducting fluoropolymer. Increasing the volume fraction of graphite to 70% also gives similar improvements in ASR and sheet resistance, but the coating does not adhere to the substrate well.

3.5. Performance of composite-coated aluminum in 3-point flexure

The stress–strain curve for a representative 3-point flexure sample is shown in Fig. 5. The deformation is elastic (or reversible) up until about a strain of 0.006, which corresponds to a flexibility of about 2%, if flexibility is defined as % deflection from mid-span, as is done in the DOE target for bipolar plates. The flexural strength of the composite-coated plates is found to be >100 MPa, exceeding the DOE target by a factor of 4. Inspection of the flexure specimens after testing with an optical microscope did not reveal damage to the coatings, which stayed well adhered to the substrate. These

Table 3
Electrochemical corrosion test results for various uncoated aluminum alloys under simulated cathodic PEM fuel cell conditions.

Alloy #	Primary alloying elements	Current density (μA cm^{-2})	Baseline R (Ω)	Final R (Ω)
2024	Cu	0.47	0.017	high
3003	Mn	0.17	0.007	0.064
3105	Mn	0.80	0.013	n/d
5052	Mg	299	0.012	10,534
6061	Mg, Si	0.14	0.009	0.087
7075	Zn	0.54	0.015	9.902

n/d: Not determined.

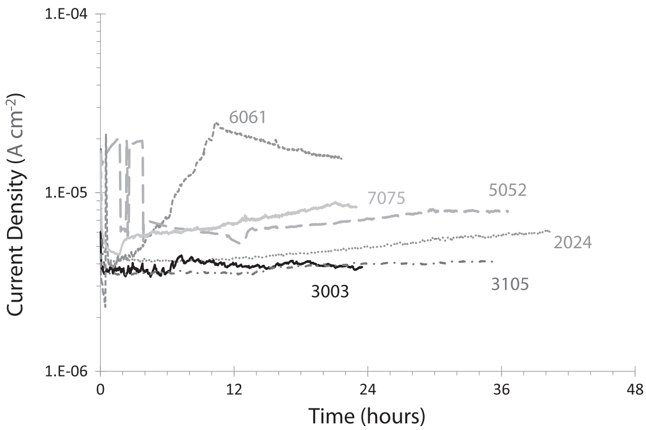

Fig. 2. Electrochemical corrosion test results for various uncoated aluminum alloys under simulated anodic PEM fuel cell conditions.

flexural tests show that the composite coatings are suitable for application in vehicles which experience many vibrations and mechanical stresses in road use.

3.6. Electrochemical corrosion of composite-coated aluminum plates

Corrosion resistance of coated aluminum samples was measured using electrochemical methods to evaluate the ability of the coatings to provide a physical barrier between the aluminum substrate and the corrosive media in a fuel cell. Typical results for aluminum plates with a coating of 25 vol% TiC/25% graphite/50 vol% EFTE applied by spraying at Orion Industries are shown in Fig. 6. The corrosion current densities for the cathodic tests were below the DOE corrosion target, however, the anodic corrosion current densities were higher than the DOE target, which is 1×10^{-6} A cm^{-2} for both anodic and cathodic conditions.

After testing, white spots were visible on the coating surface of the anodic test areas, but no spots or damage was visible on the cathodic test area. On the samples tested in cathodic conditions, it appeared that the aluminum oxide corrosion product traveled up to the surface of the coating via a defect or series of defects as if the oxide did not passivate the metal surface and corrosion continued throughout the test. The coatings did not bubble or spall off and remained adherent to the substrate after corrosion testing. For this to have occurred, there must have been pre-existing defects in the coating. The defects could arise from entrapped air bubbles or from voids left by evaporating solvents; phenomena which are difficult to avoid in the wet spray coating process. In addition, the most efficient technique for detecting defects in sprayed fluoropolymer coatings is inspection under an optical microscope, however, this is hindered when the fillers in the coating are dark colored.

When comparing the results in Fig. 6 for the coated aluminum sample to the results in Figs. 1 and 2 for uncoated 3003 aluminum, the coated 3003 aluminum had higher corrosion currents than the uncoated 3003 aluminum. The most likely reason is that the graphite in the coating promoted the corrosion of the aluminum, because graphite is more like a noble metal (i.e. has a lower "anodic index"). Had the coatings been pore-free, as they were intended to be, this would not have occurred.

Table 4
Electrochemical corrosion test results for various uncoated aluminum alloys under simulated anodic PEM fuel cell conditions.

Alloy #	Primary alloying elements	Current density (μA cm^{-2})	Baseline R (Ω)	Final R (Ω)
2024	Cu	4.99	0.017	0.031
3003	Mn	3.83	0.007	0.033
3105	Mn	3.96	0.013	0.020
5052	Mg	7.14	0.012	0.243
6061	Mg, Si	15.48	0.009	0.117
7075	Zn	8.30	0.015	0.177

Table 5
Through-thickness and in-plane electrical resistance of composite coatings.

Coating composition		ASR (Ω cm^{-2})	Sheet resistance (Ω)
Volume % fluoropolymer	Volume % fillers(s)		
30% ETFE	70% Graphite	0.47	1.8
40% ETFE	60% Graphite	0.80	3.5
40% ETFE	30% Graphite, 30% TiC	0.76	44.5
40% ETFE	40% Graphite, 20% TiC	0.52	3.2
40% ETFE	50% Graphite, 10% TiC	0.43	1.8
50% ETFE	50% Graphite	1.70	49.0
50% ETFE	25% Graphite, 25% TiC	0.37	109

3.7. Performance of composite-coated aluminum bipolar plates in single MEA tests

Fig. 7 shows the current density vs. voltage curves for 3 different coatings on stamped aluminum bipolar plates in single MEA stack tests. The performance of 50% TiC composite is much better than

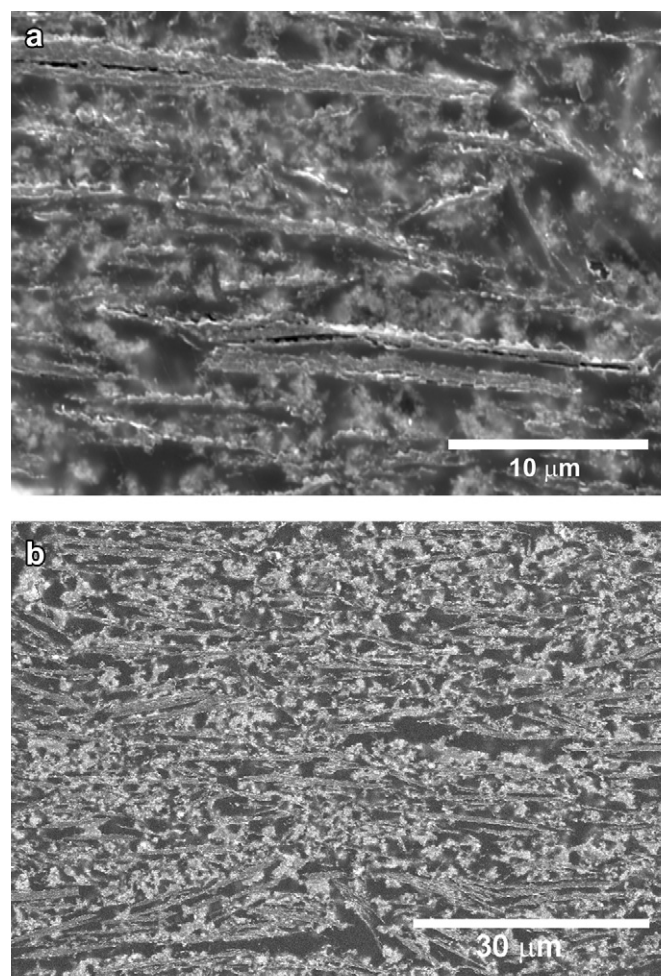

Fig. 3. SEM micrographs of the polished cross-section of a 50% PCTFE/25% graphite/25% TiC coating: (a) high magnification and (b) low magnification.

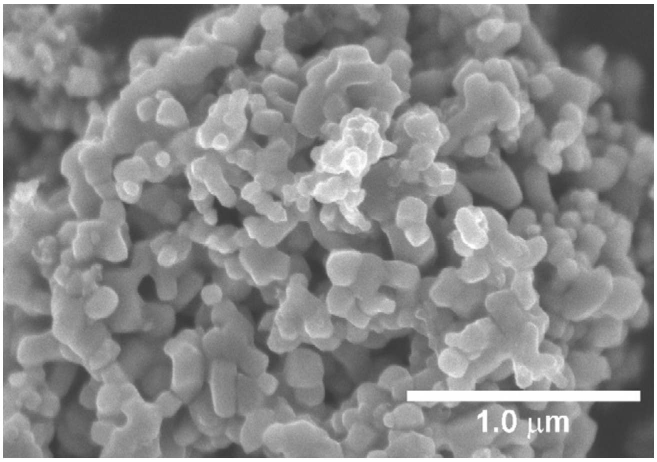

Fig. 4. SEM micrograph of as-synthesized TiC nano-powder.

that of 25%TiC/25% graphite, which indicates that coatings with high TiC content have better electrical conductivity. The 92% graphite coating showed the best performance due to the higher conductivity it possessed both in-plane and through-thickness. The performance curves in Fig. 8 show that the 90% graphite coating performed better than uncoated aluminum because the uncoated aluminum had a resistive passivating oxide layer on the surface. For the coated samples, the passivating layer was removed prior to coating application and the coating effectively prevented it from forming again at ambient conditions. The coated sample did become more resistive during testing and performance quickly dropped.

Our tests show that a pinhole-free coating is absolutely necessary to protect the aluminum bipolar plate from corrosion, particularly under anodic simulated PEM fuel cell conditions. Since sprayed composite coatings have a greater tendency to retain porosity after sintering as compared to neat fluoropolymer coatings, an improved application method needs to be identified. The use of a composite coating may need to be coupled with a pretreatment of the aluminum plate to deposit a conversion coating layer [20,23] that improves corrosion resistance. An alternative coating application method may also be needed to improve electrical conductivity because spraying yields graphite platelets oriented parallel to the substrate rather than perpendicular. Although, having the graphite platelets oriented parallel to the substrate on the exposed surface is advantageous to the surface conductivity.

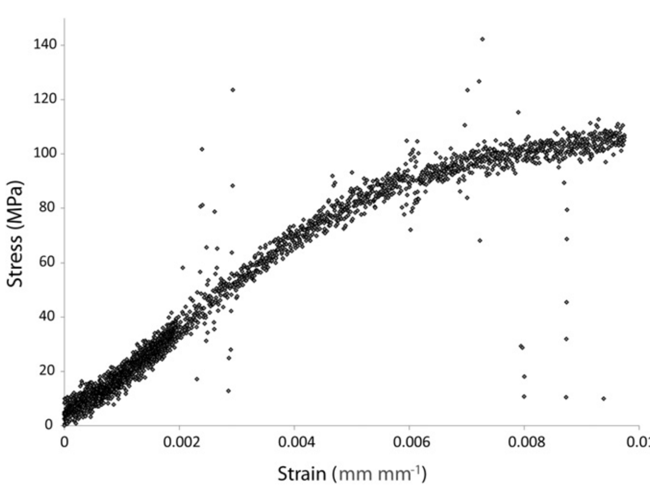

Fig. 5. 3-point flexure test results for a (50% ETFE/25% TiC/25% graphite) coating on 3003 aluminum.

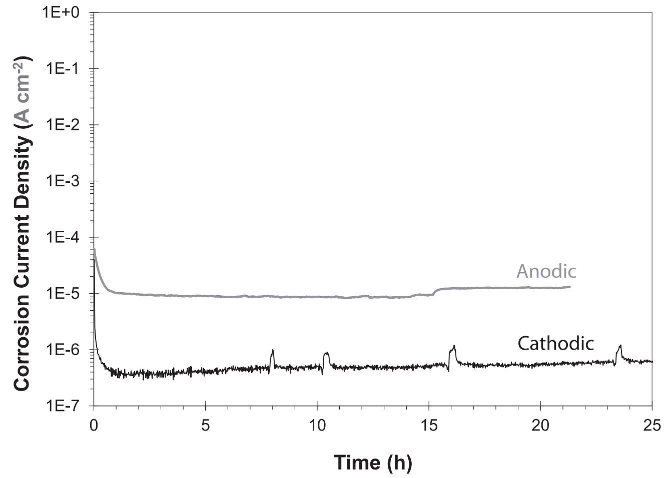

Fig. 6. Electrochemical corrosion test results for (50% ETFE/25% TiC/25% graphite) coated 3003 aluminum under simulated fuel cell conditions.

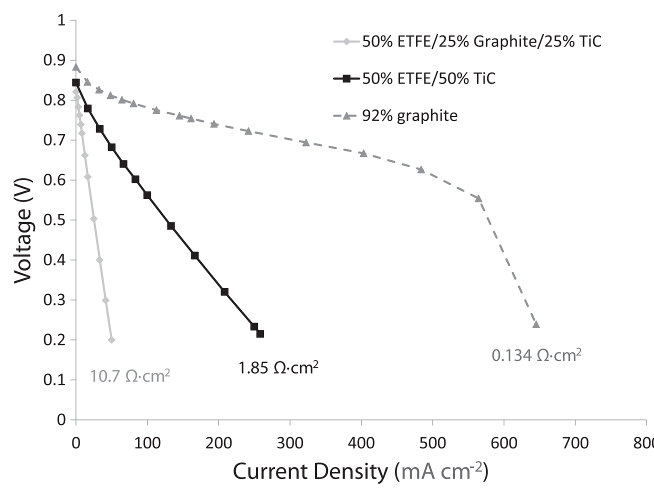

Fig. 7. Single MEA test results for three different coatings on 3105 aluminum.

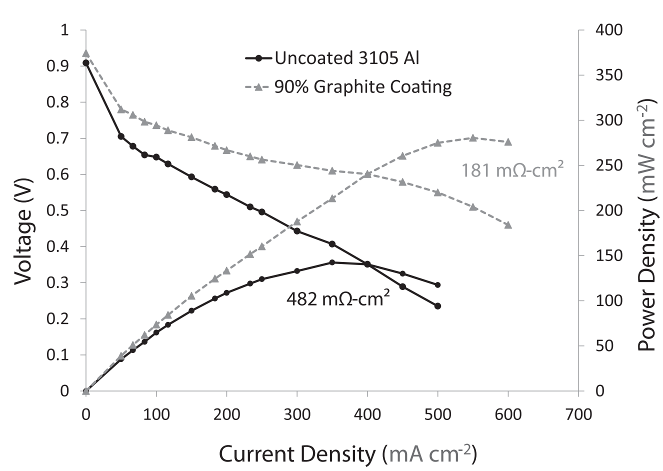

Fig. 8. Single MEA test results for uncoated vs. coated aluminum.

4. Conclusions

Aluminum bipolar plates offer potential weight reduction over stainless steel bipolar plates, however, a pinhole-free, acid-resistant, electrically conductive, damage-resistant coating is needed. Our strategy was to use wet spraying to apply a composite coating of an electrically conductive filler materials and a fluoropolymer. We conducted acid stability and electrochemical stability tests which showed that graphite and TiC were the most suitable electrically conductive filler materials. Using these two fillers with ETFE, we were able to achieve the DOE target for in-plane conductivity, but not through-thickness ASR. The wet spraying application method aided the surface conductivity, but inhibited the through-thickness conductivity by causing a layered microstructure to form. Specifically, the conductive graphite platelets were left oriented parallel to the surface of the aluminum substrate with non-conductive fluoropolymer in-between graphite layers. Replacing some of the graphite with TiC helped because it was more isotropic and fit in between the graphite layers increasing the number of continuous electrical paths from the surface to the substrate. Replacing too much of the graphite decreased the in-plane surface conductivity too much because there was no longer a continuous network of graphite platelets lying on the free surface of the coating. The composite-coated aluminum plates also survived 3-point flexure tests exhibiting flexural strength greater than 100 MPa and a flexibility of 2%. 3000 series aluminum alloys were found to have the best corrosion resistance in our electrochemical corrosion tests on uncoated aluminum alloys. The composite-coated aluminum samples were able to meet the DOE corrosion target for cathodic conditions, but not for anodic conditions. Those results indicate that we were not able to achieve a pinhole-free coating using wet spraying as the coating application method. Using dark-colored filler materials made pinholes in the coating difficult to detect because optical methods are typically used by the fluoropolymer coatings industry to inspect coatings for defects. Another application method for the composite coatings that can eliminate pinholes needs to be identified.

Acknowledgments

The authors would like to thank Dileep Singh of the Nuclear Energy Division at Argonne for his assistance in using the mechanical testing machine. Also, we would like to thank Terry Cruse, Nathan Styx, T. Keith Honaker-Schroeder, Sarah Stariha, Nancy Dietz-Rago, Jack Vaughey, Brian Ingram, Vic Maroni, Deborah Myers, and Romesh Kumar of the Chemical Sciences and Engineering Division at Argonne for their valuable support and assistance. ICP-OES was carried out by Don Graczyk and Seema Naik, and of the Analytical Chemistry Laboratory at Argonne National Laboratory. Scanning electron microscopy was carried out at the Analytical Chemistry Laboratory and the Electron Microscopy Center at Argonne National Laboratory. Funding was provided by the U.S. Department of Energy, Office of Energy Efficiency and Renewable Energy, Fuel Cell Technology Program.

References

[1] B.D. James, J.A. Kalinoski, K.N. Baum, Mass Production Cost Estimation for Direct H_2 PEM Fuel Cell Systems for Automotive Applications: 2010 Update, Directed Technologies, Arlington, VA, 2010.
[2] N.D.L. Heras, E.P.L. Roberts, R. Langton, D.R. Hodgson, Energy Environmental Science 2 (2009) 206–214.
[3] C. Davies, M. Barnett, Journal of Organic Materials 56 (2004) 22–24.
[4] Fuel Cell Technologies Program Multi-Year Research, Development and Demonstration Plan, U.S. Department of Energy, Office of Energy Efficiency and Renewable Energy, Fuel Cell Technologies Program, Washington DC, 2011.
[5] G.V. Samsonov, I.M. Vinitskii, Handbook of Refractory Compounds, IFI/Plenum, New York, NY, 1980.
[6] R. Koc, J.S. Folmer, Journal of Materials Science 32 (1997) 3101–3111.
[7] R. Koc, G. Glatzmaier, Process for Synthesizing Titanium Carbide, Titanium Nitride, and Titanium Carbonitride, U.S. Patent 5,417,952 (1995).
[8] R. Koc, D.B. Hodge, Journal of Materials Science Letters 19 (2000) 667–669.
[9] R. Duddukuri, R. Koc, J. Mawdsley, D. Carter, Synthesis of nano-size TiB2 powders using carbon coated precursors, in: Nanostructured Materials and Nanotechnology, vol. V, John Wiley & Sons, Inc., 2011, pp. 165–175.
[10] N. Siddiqui, R. Koc, J. Mawdsley, D. Carter, Synthesis of submicron/nano sized CaB_6 from carbon coated precursors, in: Nanostructured Materials and Nanotechnology, vol. V, John Wiley & Sons, Inc., 2011, pp. 137–149.
[11] D. Knigge, T. Jacksier, E. Claude, A. Milahi-SC, Electrochemical Corrosion Testing and In-Stack Aging of Metallic Bipolar Plates for PEM Fuel Cells, Proceedings of the 16th World Hydrogen Energy Conference, Lyon, France, 2006.
[12] Y. Soma, I. Muto, N. Hara, Materials Transactions 51 (2010) 939–947.
[13] K.S. Weil, G. Xia, Z.G. Yang, J. Kim, International Journal of Hydrogen Energy 32 (2007) 3724–3733.
[14] H.S. Choi, D.H. Han, W.H. Hong, J.J. Lee, Journal of Power Sources 189 (2009) 966–971.
[15] H. Yu, L. Yang, L. Zhu, X. Jian, Z. Wang, L. Jiang, Journal of Power Sources 191 (2009) 495–500.
[16] J.D. Carter, J.R. Mawdsley, S.G. Niyogi, T.A. Cruse, X. Wang, L. Santos, Corrosion Resistant Bipolar Plate for Polymer Electrolyte Fuel Cells, U.S. Patent 7699916, 2010.
[17] H.L. Wang, M.A. Sweikart, J.A. Turner, Journal of Power Sources 115 (2003) 243–251.
[18] B. Avasarala, P. Haldar, Journal of Power Sources 188 (2009) 225–229.
[19] L.G. Marianowski, Sheet Metal Bipolar Plate Design for Polymer Electrolyte Membrane Fuel Cells, US Patent 6,261,710, 2001.
[20] J.J. Zhang, W.F. Li, J. Du, D. Han, X.P. Zheng, Chinese Science Bulletin 55 (2010) 3345–3349.
[21] J.M. Sykes, I. Danilidis, J. Hunter, G.M. Scamans, Corrosion Science 49 (2007) 1559–15691569.
[22] Engineered Materials Handbook, , In: Ceramics and Glasses, vol. 4, ASM International, 1991.
[23] F. Mansfeld, Y. Wang, H. Shih, Electrochimica Acta 37 (1992) 2277–2282.